Pergamon

Int. J. Solids Structures Vol. 31, No. 8, pp. 1085–1097, 1994

0020–7683/94 $6.00 + .00

THE DYNAMIC INTERACTION OF A MICROCRACK WITH A MAIN CRACK UNDER ANTIPLANE LOADING

S. A. MEGUID and X. D. WANG
Engineering Mechanics and Design Laboratory, Department of Mechanical Engineering, University of Toronto, Ontario, Canada M5S 1A4

(*Received* 2 *June* 1993; *in revised form* 27 *October* 1993)

Abstract—A comprehensive theoretical treatment is given of the dynamic interaction between a main crack and an *arbitrarily* located and oriented microcrack near its tip under antiplane loading. The theoretical formulations governing the steady-state problem are based upon the use of integral transform techniques and an appropriate superposition procedure. The resulting singular integral equations are solved numerically, using Chebyshev polynomials, to provide the dynamic stress intensity factor at the main crack at different loading frequencies. The resulting solution is verified by comparison with existing results and numerical examples are provided to show the effect of the location and orientation of the microcrack and the frequency upon the dynamic stress intensity factor of the main crack.

1. INTRODUCTION

The interaction of cracks with microcracks plays an important role in the mechanics and micromechanics of fracture in quasi-brittle solids such as concrete, rock and ceramics. Existing work in the literature suggests that the presence of these defects ultimately governs the overall failure mechanism of these solids; see, for example, Hoagland *et al.* (1973, 1980), Claussen *et al.* (1977), Evans and Faber (1984) and Ruhle *et al.* (1987). Indeed, an accurate assessment of the toughness of such materials would necessitate the determination of the influence of these microdefects upon the crack-tip stress field.

Two approaches are generally considered in modelling the quasi-static interaction problem. The first utilizes the mechanics of continuum damage to model a zone in the vicinity of the main crack. In this case, the damage zone is described on the basis of phenomenological constitutive equations different from that corresponding to the behavior of the original material (Krajcinovic, 1985; Ortiz, 1987; Hutchinson, 1987). The second relies upon the use of a fundamental micromechanics approach to model multiple discrete microdefects near the tip of the main crack (Kachanov, 1987; Rose, 1986; Meguid *et al.*, 1991; Gong and Meguid, 1991).

In spite of the fact that the quasi-static main crack–microcrack interaction problem has received considerable attention, only a very limited number of articles treat the dynamic interaction between collinear or parallel cracks; see, for example, Jain and Kanwal (1972), Itou (1980), Gross and Zhang (1988), Zhang and Achenbach (1989) and Zhang (1992). This may be due partly to the difficulties associated with the formulations resulting from the dynamic equations and partly to the scarcity of experimental data. It is important to note, however, that most advanced composite materials are currently being used in situations involving dynamic loading rather than static ones.

It is therefore the objective of this paper to provide a steady-state solution to the dynamic interaction between a main crack and an *arbitrarily* located and oriented microcrack subjected to different loading frequency. The analysis is based upon the use of Fourier integral transforms and an appropriate superposition procedure using Chebyshev polynomials. Two aspects of the work are accordingly examined. The first is concerned with determining the effect of the loading frequency upon the resulting dynamic stress intensity factor, while the second is associated with the possible shielding and amplification effects observed in the equivalent static problem.

The general layout of this article is as follows: Section 2 provides the general formulation of the problem, while Section 3 is devoted totally to the analysis of results and discussions. Section 4 concludes the paper.

SAS 31:8-D

2. FORMULATION OF THE PROBLEM

2.1. *Decomposition into subproblems*

The situation envisaged is that of an elastic infinitely extended isotropic solid containing a main crack and an arbitrarily located and oriented microcrack under steady-state dynamic antiplane loading, as shown in Fig. 1. The main crack is assumed to be semi-infinite, which corresponds to the assumption that the length of the main crack is much larger than the length of the microcrack $2a$ and the distance between the main crack and the microcrack. Two rectangular coordinate systems (x, y) and (ξ, η) are employed at the semi-infinite main crack and the microcrack, respectively. Let the distance between the main crack-tip and the centre of the microcrack denoted d and the inclination angle measured from the x-axis to the centre of the microcrack θ. The microcrack orientation angle ϕ is measured from the x-axis to the ξ-axis.

The displacement, strain and stress fields corresponding to a steady-state dynamic loading can be expressed in terms of the frequency ω as

$$A^*(x, y, t) = A(x, y)\, e^{i\omega t}, \tag{1}$$

where A^* represents the desired field variable. For the sake of convenience, the time factor $\exp(i\omega t)$ will be suppressed and only $A(x, y)$ will be considered.

The solution to the current dynamic problem is obtained by superimposing three subproblems, each of which contains either the main crack or the microcrack. In subproblem I, the main crack is subjected to the applied dynamic shear stress which results in a shear stress field at the microcrack site. In subproblem II, the presence of the microcrack in the infinite body results in a shear stress distribution at the main crack site. In subproblem III, the main crack surfaces are subjected to an equal and opposite shear stress experienced in subproblem II. This stress field will again introduce a shear stress distribution at the microcrack site which should be added to the field corresponding to subproblem II. This iterative process is repeated until it converges to the "exact" solution of the problem. The formal representation of the above approach is described below.

In subproblem I, the externally applied dynamic loads result in the following stress field

$$\tau_{\beta z} = \frac{K_0}{\sqrt{2\pi r}} \cos\left(\frac{\beta}{2}\right) + p_2 \cos(\beta) + p_3 r^{1/2} \cos\left(\frac{3\beta}{2}\right) + p_4 r \cos(2\beta) + \cdots \tag{2}$$

$$\tau_{rz} = -\frac{K_0}{\sqrt{2\pi r}} \sin\left(\frac{\beta}{2}\right) + p_2 \sin(\beta) + p_3 r^{1/2} \sin\left(\frac{3\beta}{2}\right) + p_4 r \sin(2\beta) + \cdots \tag{3}$$

at a point (r, β) in the neighbourhood of the main crack tip, with K_0 being the applied stress intensity factor and $p_2, p_3, \ldots$ are parameters corresponding to the higher order terms of the stress field. The use of higher order terms in (2) and (3) was motivated by the knowledge that the stress field at the microcrack site is not merely governed by the singular stress field at the main crack (Gong and Meguid, 1992).

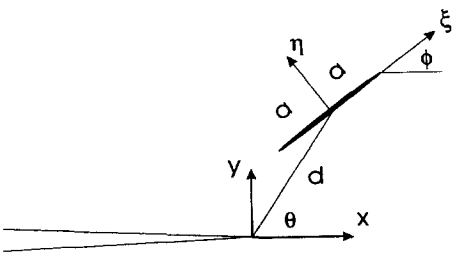

Fig. 1. Arbitrarily located and oriented microcrack near the tip of a main crack.

Consequently, the shear stress $\tau_1(\xi)$ along the microcrack site can be described in terms of the undisturbed stress field as being

$$\tau_1(\xi) = \tau_{yz}(r, \beta)\cos\phi - \tau_{xz}(r, \beta)\sin\phi \tag{4}$$

with

$$\tau_{yz}(r, \beta) = \tau_{rz}(r, \beta)\sin\beta + \tau_{\beta z}(r, \beta)\cos\beta \tag{5}$$

and

$$\tau_{xz}(r, \beta) = \tau_{rz}(r, \beta)\cos\beta - \tau_{\beta z}(r, \beta)\sin\beta, \tag{6}$$

where

$$r = \sqrt{x^2+y^2}, \quad \beta = \arctan\left(\frac{y}{x}\right) \tag{7}$$

and

$$x = d\cos(\theta) + \xi\cos(\phi), \quad y = d\sin(\theta) + \xi\sin(\phi). \tag{8}$$

In subproblem II, the microcrack is subjected to $-\tau_1$ and its elastodynamic behaviour, under steady-state antiplane deformation, is governed by the following equation (Achenbach, 1973)

$$\frac{\partial^2 w}{\partial \xi^2} + \frac{\partial^2 w}{\partial \eta^2} + \frac{\omega^2}{c^2} w = 0, \tag{9}$$

where w, ω and c are the displacement, the frequency and the velocity of the transverse wave of the material, respectively. The non-vanishing shear stress components are

$$\tau_{\eta z} = G\frac{\partial w}{\partial \eta}, \quad \tau_{\xi z} = G\frac{\partial w}{\partial \xi}, \tag{10}$$

where G is the shear modulus of the material. By making use of Fourier transforms (see the Appendix for details), the general solution of the wave equation (9) can be expressed in terms of the following Fourier integrals

$$w(\xi, \eta) = \operatorname{sgn}(\eta)\int_{-\infty}^{\infty} A(s)\,e^{-\alpha|\eta| - is\xi}\,ds, \tag{11}$$

$$\tau_{\eta z}(\xi, \eta) = -G\int_{-\infty}^{\infty} \alpha A(s)\,e^{-\alpha|\eta| - is\xi}\,ds, \tag{12}$$

$$\tau_{\xi z}(\xi, \eta) = -iG\operatorname{sgn}(\eta)\int_{-\infty}^{\infty} sA(s)\,e^{-\alpha|\eta| - is\xi}\,ds, \tag{13}$$

where

$$\operatorname{sgn}(\eta) = \begin{cases} 1, & \eta > 0 \\ -1, & \eta < 0. \end{cases}$$

In the above equations, $A(s)$ is an unknown function of s, and α is given by

$$\alpha = \sqrt{s^2 - \frac{\omega^2}{c^2}} \quad \text{with} \quad \operatorname{Re}(\alpha) \geqslant 0 \tag{14}$$

which ensures that the stress field induced by the microcrack satisfies the boundary conditions of the problem at infinity.

By introducing the following dislocation density function

$$f(\xi) = \frac{\partial w(\xi, 0)}{\partial \xi} \tag{15}$$

the unknown function $A(s)$ can be found as

$$A(s) = -\frac{\bar{f}(s)}{\mathrm{i}s}, \tag{16}$$

where

$$\bar{f}(s) = \frac{1}{2\pi} \int_{-\infty}^{\infty} f(\xi)\, \mathrm{e}^{\mathrm{i}s\xi}\, \mathrm{d}\xi \tag{17}$$

is the Fourier transform of $f(\xi)$. Substitution of eqns (16) and (17) into eqns (11)–(13) yields

$$w(\xi, \eta) = -\frac{\operatorname{sgn}(\eta)}{2\pi \mathrm{i}} \int_{-\infty}^{\infty} f(u) \int_{-\infty}^{\infty} \frac{1}{s} \mathrm{e}^{\mathrm{i}s(u-\xi) - \alpha|\eta|}\, \mathrm{d}s\, \mathrm{d}u \tag{18}$$

$$\tau_{\eta z}(\xi, \eta) = -\frac{G}{2\pi \mathrm{i}} \int_{-\infty}^{\infty} f(u) \int_{-\infty}^{\infty} \frac{\alpha}{s} \mathrm{e}^{\mathrm{i}s(u-\xi) - \alpha|\eta|}\, \mathrm{d}s\, \mathrm{d}u \tag{19}$$

$$\tau_{\xi z}(\xi, \eta) = -\frac{G \operatorname{sgn}(\eta)}{2\pi \mathrm{i}} \int_{-\infty}^{\infty} f(u) \int_{-\infty}^{\infty} \frac{1}{s} \mathrm{e}^{\mathrm{i}s(u-\xi) - \alpha|\eta|}\, \mathrm{d}s\, \mathrm{d}u. \tag{20}$$

The microcrack is subjected to the following boundary conditions

$$w(\xi, 0) = 0, \quad |\xi| \geqslant a; \quad \tau_{\eta z}(\xi, 0) = -\tau_1(\xi), \quad |\xi| < a. \tag{21}$$

By using eqns (18) and (19) in (21), the above boundary conditions can be expressed in terms of the following singular integral equations

$$\int_{-a}^{a} \frac{f(u)}{u-\xi}\, \mathrm{d}u + \int_{-a}^{a} f(u) \int_{0}^{\infty} \left[\frac{\alpha}{s} - 1\right] \sin[s(u-\xi)]\, \mathrm{d}s\, \mathrm{d}u = -\frac{\pi}{G} \tau_1(\xi), \quad |\xi| < a \tag{22}$$

and

$$\int_{-a}^{a} f(u)\, \mathrm{d}u = 0. \tag{23}$$

Equations (22) and (23) can be solved by expanding $f(u)$ using Chebyshev polynomials; as follows:

$$f(u) = \sum_{j=0}^{\infty} \frac{c_j}{\sqrt{1-\frac{u^2}{a^2}}} T_j\left(\frac{u}{a}\right), \tag{24}$$

where T_j are Chebyshev polynomials of the first kind and c_j are unknown constants. From the orthogonality conditions of the Chebyshev polynomials, eqn (23) reduces to $c_0 = 0$. Substituting (24) into (22) and making use of the following relations ($p > 0$)

$$\int_{-1}^{1} (1-u^2)^{-1/2} T_k(u) \sin(pu)\, du = \begin{cases} 0 & k = 2n \\ (-1)^n \pi J_k(p) & k = 2n+1 \end{cases} \tag{25}$$

$$\int_{-1}^{1} (1-u^2)^{-1/2} T_k(u) \cos(pu)\, du = \begin{cases} 0 & k = 2n+1 \\ (-1)^n \pi J_k(p) & k = 2n \end{cases} \tag{26}$$

with J_k being Bessel functions of the first kind; the following algebraic equation for c_j is obtained

$$\sum_{j=1}^{\infty} c_j U_{j-1}\left(\frac{\xi}{a}\right) + \sum_{j=1}^{\infty} c_j g_j(\xi) = -\tau_1(\xi)/G, \quad |\xi| < a, \tag{27}$$

where U_j represent Chebyshev polynomials of the second kind with

$$g_j(\xi) = \begin{cases} (-1)^n a \int_0^{\infty} \left(\frac{\alpha}{s} - 1\right) J_j(sa) \cos(s\xi)\, ds, & j = 2n+1 \\ (-1)^{(n+1)} a \int_0^{\infty} \left(\frac{\alpha}{s} - 1\right) J_j(sa) \sin(s\xi)\, ds, & j = 2n. \end{cases} \tag{28}$$

If the Chebyshev polynomials in eqn (24) are truncated to the Nth term and eqn (27) is satisfied at N collocation points given by

$$\xi_l = a \cos\left(\frac{l}{N+1}\pi\right), \quad l = 1, 2, \ldots, N \tag{29}$$

then eqn (27) reduces to the following linear algebraic equations

$$\sum_{j=1}^{N} c_j \frac{\sin\left(\frac{jl\pi}{N+1}\right)}{\sin\left(\frac{j\pi}{N+1}\right)} + \sum_{j=1}^{N} c_j g_j(\xi_l) = -\tau_1(\xi_l)/G, \quad j, l = 1, 2, \ldots, N. \tag{30}$$

The solution for c_j ($j = 1, 2, \ldots, N$) can be obtained from these equations. Once c_j are determined, the stress distribution resulting from the presence of the microcrack can be expressed as

$$\tau_{\eta z}(\xi,\eta) = Ga\sum_{j=1}^{N} c_j \begin{cases} (-1)^n \int_0^\infty \frac{\alpha}{s} J_j(sa)\cos(s\xi)\,e^{-\alpha|\eta|}\,ds, & j=2n+1 \\ (-1)^{(n+1)} \int_0^\infty \frac{\alpha}{s} J_j(sa)\sin(s\xi)\,e^{-\alpha|\eta|}\,ds, & j=2n \end{cases} \tag{31}$$

and

$$\tau_{\xi z}(\xi,\eta) = Ga\,\mathrm{sgn}(\eta)\sum_{j=1}^{N} c_j \begin{cases} (-1)^{(n+1)} \int_0^\infty J_j(sa)\sin(s\xi)\,e^{-\alpha|\eta|}\,ds, & j=2n+1 \\ (-1)^n \int_0^\infty J_j(sa)\cos(s\xi)\,e^{-\alpha|\eta|}\,ds, & j=2n. \end{cases} \tag{32}$$

Let us now focus our attention to subproblem III, where the stress field at the main crack, resulting from the microcrack, can be expressed as

$$\tau_1^M(x) = \tau_{\xi z}[\bar{\xi}(x),\bar{\eta}(x)]\sin\phi + \tau_{\eta z}[\bar{\xi}(x),\bar{\eta}(x)]\cos\phi \tag{33}$$

with

$$\bar{\xi}(x) = (x - d\cos\theta)\cos\phi + d\sin\theta(\cos\phi+1)\frac{\cos\phi-1}{\sin\phi} \tag{34}$$

and

$$\bar{\eta}(x) = (d\cos\theta - x)\sin\phi - d\sin\theta\cos\phi. \tag{35}$$

It is now appropriate to free the main crack from the induced shear stress by applying $-\tau_1^M(x)$ to its surfaces. Knowledge of the solution for the transient mode III semi-infinite crack problem (Freund, 1990) leads to the development of the following expression of the stress field for the steady-state case

$$\tau_{yz}(r,0) = \frac{K_1}{\sqrt{2\pi r}} - \frac{\sqrt{r}}{\pi}\int_0^\infty \frac{\tau_1^M(-u)}{\sqrt{u}(r+u)} e^{-iku}\,du \tag{36}$$

$$K_1 = \sqrt{\frac{2}{\pi}}\int_0^\infty \frac{\tau_1^M(-u)}{\sqrt{u}} e^{-iku}\,du, \tag{37}$$

where $k = \omega/c$ is the wave number, K_1 is the first-order effect of the microcrack on the stress intensity factor of the main crack.

2.2. *Superposition of subproblems*

Equation (36) can be expressed in an expanded form as follows:

$$\tau_{yz}(r,0) = \tau_{\beta z}(r,0) = \alpha_1 r^{-1/2} + \alpha_2 + \alpha_3 r^{1/2} + \alpha_4 r + \cdots \tag{38}$$

which if compared with eqn (2) gives

$$K_1 = \sqrt{2\pi}\alpha_1, \quad p_2^1 = \alpha_2, \quad p_3^1 = \alpha_3, \quad p_4^1 = \alpha_4 \cdots. \tag{39}$$

Accordingly, the stress field of the main crack for the next iteration can be obtained from eqn (2) with K_0 and $p_2, p_3, \ldots$ being replaced by K_1 and $p_2^1, p_3^1, \ldots$, respectively. In fact, the stress field of the main crack in eqn (2) is governed by the stress parameters

$p_1, p_2, p_3, \ldots$, with $p_1 = K_0/\sqrt{2\pi}$. Generally, only a finite number of terms involving $p_1, p_2, \ldots, p_m$ will be used to achieve a desired accuracy. In view of the linear elastic property of the system, the relation between the stress parameters for different iteration orders can be expressed as

$$\begin{bmatrix} p_1^{j+1} \\ p_2^{j+1} \\ \vdots \\ p_m^{j+1} \end{bmatrix} = \begin{bmatrix} \alpha_{11} & \alpha_{12} & \ldots & \alpha_{1m} \\ \alpha_{21} & \alpha_{22} & \ldots & \alpha_{2m} \\ & & \ldots & \\ \alpha_{m1} & \alpha_{m2} & \ldots & \alpha_{mm} \end{bmatrix} \begin{bmatrix} p_1^j \\ p_2^j \\ \vdots \\ p_m^j \end{bmatrix}, \tag{40}$$

where p_l^j ($l = 1, 2, \ldots, m$) are the stress parameters of the main crack with j being the order of iteration and $[\alpha]$ being the coefficient matrix which is governed by the geometric and the frequency conditions of the problem.

The iterative solution of (40) leads to

$$\mathbf{p}^j = [\alpha]^j \mathbf{p}^0, \tag{41}$$

where $\mathbf{p}^j$ and $\mathbf{p}^0$ are the stress parameters for jth and the initial iterations, respectively. The final result of the stress parameters $\mathbf{p}$ can thus be obtained using the following sum

$$\mathbf{p} = \mathbf{p}^0 + \mathbf{p}^1 + \mathbf{p}^2 + \mathbf{p}^3 + \cdots + \mathbf{p}^j + \cdots \tag{42}$$

which can be expressed in terms of $[\alpha]$ as

$$\mathbf{p} = (\mathbf{I} + [\alpha] + [\alpha]^2 + \cdots + [\alpha]^j + \cdots)\mathbf{p}^0. \tag{43}$$

Since the eigenvalues of matrix $[\alpha]$ are less than one, then the sum of (43) can be rewritten as

$$\mathbf{p} = \mathbf{q}\mathbf{p}^0, \tag{44}$$

where

$$\mathbf{q} = (\mathbf{I} - [\alpha])^{-1}. \tag{45}$$

If the initially applied stress intensity factor at the main crack is K_0 ($p_1 = K_0/\sqrt{2\pi}$; $p_l = 0$, $l > 1$), then the stress intensity factor at the main crack tip in the presence of the microcrack is given by

$$K_{III} = q_{11} K_0 \quad \text{or} \quad K^* = \frac{K_{III}}{K_0} = q_{11}. \tag{46}$$

3. RESULTS AND DISCUSSION

This section is divided into two main parts. The first deals with the verification of the resulting solutions and the second with examining the effect of the pertinent parameters upon the stress intensity factor at the main crack.

The following forms of solutions were utilized in the determination of the normalized stress intensity factor of the main crack:

(i) the first-order solution, $K^{(1)} = 1 + \alpha_{11}$,
(ii) the singular field solution $K^{\sin} = 1/(1 - \alpha_{11})$ and
(iii) the higher order solution, $K^* = q_{11}$ with $\mathbf{q} = (\mathbf{I} - [\alpha])^{-1}$.

Table 1. Normalized quasi-static stress intensity factor at the tip of the main crack K_{III}/K_0 as a function of location a/d for $\theta = \phi = 90^\circ$

	Gong and Meguid (1991)		Present result		
a/d	First order	Second order	$1+\alpha_{11}$	$1/(1-\alpha_{11})$	q_{11}
0.0	1.000	1.000	1.000	1.000	1.000
0.1	1.001	1.001	1.001	1.001	1.001
0.2	1.005	1.005	1.003	1.003	1.003
0.3	1.011	1.012	1.006	1.006	1.006
0.4	1.020	1.023	1.011	1.011	1.012
0.5	1.031	1.039	1.021	1.021	1.022
0.6	1.045	1.060	1.038	1.039	1.040
0.7	1.061	1.089	1.067	1.072	1.074
0.8	1.080	1.128	1.119	1.136	1.142
0.9	1.101	1.177	1.233	1.304	1.333

First, we restrict our attention to the static case ($\omega = 0$) for which a general solution has been found by Gong and Meguid (1991) using the complex variable method and Laurent series expansion. The results of the normalized stress intensity factor of the main crack given by Gong and Meguid are compared with the results of the present solution in Table 1 for $\theta = \phi = 90^\circ$. In addition, comparison is also made in Table 2 with the special case of collinear cracks for which an exact solution exists (Chiang, 1986). These tables reveal that: (i) the accuracy of the solution is governed by the relative position of the microcrack, a/d, and (ii) a maximum discrepancy of 5% is observed if the number of Chebyshev polynomials in eqn (24) was restricted to eight and the number of stress parameters in eqn (40) to four, even for the case where $a/d = 0.9$.

Furthermore, the accuracy of the solution was verified using the case of a single crack subjected to a uniform harmonic shear stress developed earlier by Gross and Zhang (1988). Figure 2 shows an excellent agreement between the present solution and those of Gross and Zhang in which the normalized dynamic stress intensity factor was defined as being $K = K_{III}/K^s_{III}$, with K^s_{III} being the corresponding static stress intensity factor and ka the normalized wave number. For the remainder of this paper, only the higher order solution will be considered in the analysis of results.

Consider now the case of an arbitrarily located and oriented microcrack ahead of the main crack. The present formulations predict the dependence of the normalized stress intensity factor upon the location (a/d, θ) and orientation of the microcrack (ϕ) and the frequency (ω). It should be recognized that the dynamic stress intensity factor produced by a time-harmonic loading is in general a complex quantity. For convenience, only the amplitude of the normalized complex dynamic stress intensity factor $|K^*|$ is considered in the following figures.

Figure 3(a) shows the variation of $|K^*|$ with the frequency for different a/d for the collinear crack case. The figure shows that $|K^*|$ attains a maximum amplitude at zero frequency. However, as the normalized wave number ka increases and reaches 1.5, the

Table 2. Normalized quasi-static stress intensity factor at the tip of the main crack K_{III}/K_0 as a function of location a/d for collinear cracks

		Gong and Meguid (1991)		Present result		
a/d	Exact	First order	Second order	$1+\alpha_{11}$	$1/(1-\alpha_{11})$	q_{11}
0.0	1.000	1.000	1.000	1.000	1.000	1.000
0.1	1.003	1.003	1.003	1.002	1.002	1.002
0.2	1.010	1.010	1.010	1.007	1.009	1.009
0.3	1.024	1.022	1.024	1.017	1.022	1.021
0.4	1.046	1.040	1.045	1.034	1.043	1.042
0.5	1.077	1.063	1.074	1.060	1.076	1.073
0.6	1.123	1.090	1.113	1.099	1.129	1.112
0.7	1.195	1.123	1.166	1.161	1.221	1.195
0.8	1.319	1.160	1.234	1.266	1.413	1.331
0.9	1.591	1.203	1.320	1.492	2.103	1.678

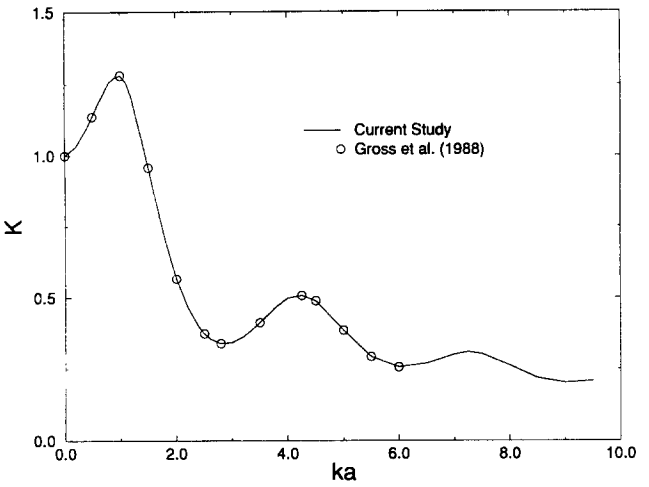

Fig. 2. Verification of present solution for a crack under dynamic loading.

normalized stress intensity factor $|K^*|$ decreases rapidly and approaches unity. Similar behaviour was observed for other cases corresponding to arbitrarily located and oriented microcracks; as shown, for example, in Fig. 3(b) for the case $\theta = \phi = 90°$. Figures 3(a) and 3(b) indicate that the effect of the microcrack in the current configuration is significantly reduced at higher frequencies.

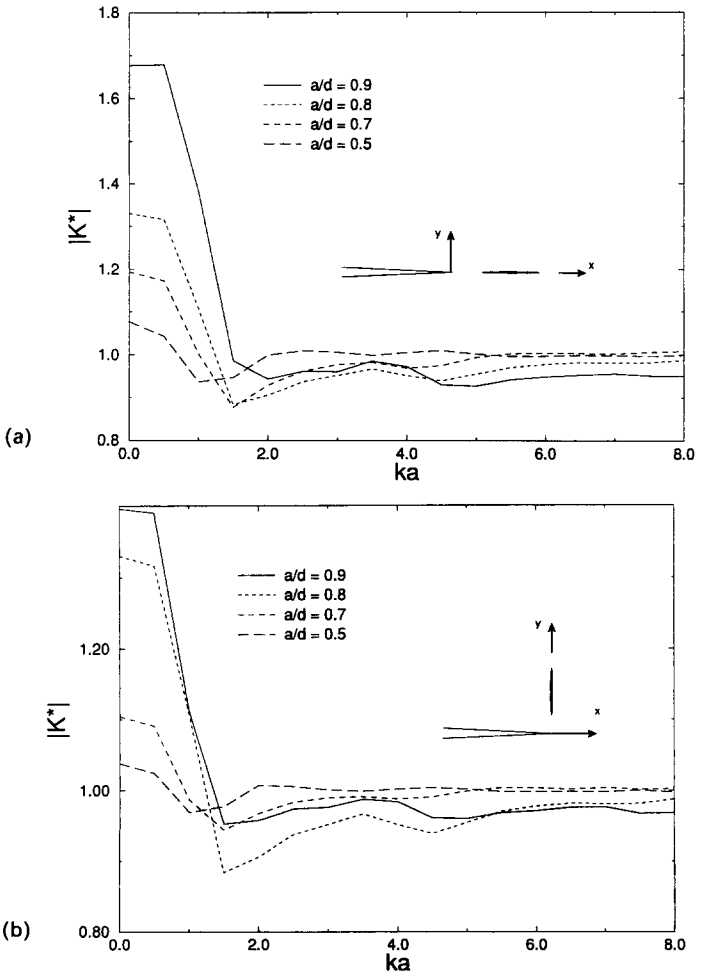

Fig. 3. Variation of normalized dynamic stress intensity factor K^* versus normalized wave number ka for different locations of microcrack a/d: (a) $\theta = \phi = 0°$ and (b) $\theta = \phi = 90°$.

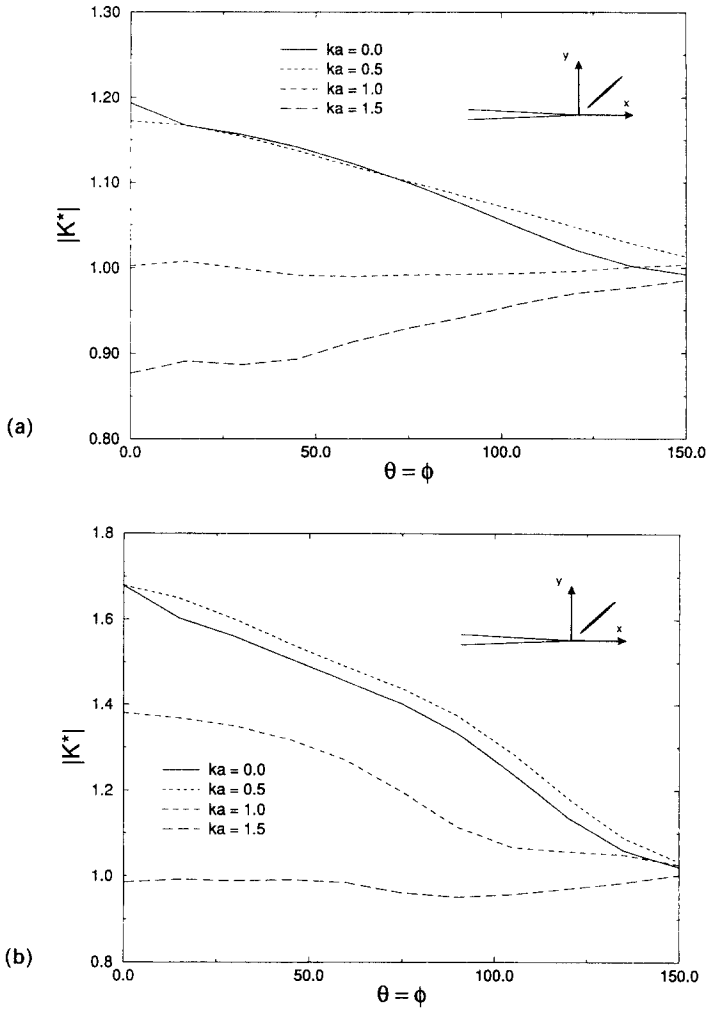

Fig. 4. Effect of microcrack inclination θ upon the dynamic stress intensity factor K^* for different frequencies: (a) $a/d = 0.7$ and (b) $a/d = 0.9$.

Figures 4(a) and 4(b) show the variation of $|K^*|$ with the inclination angle θ, which is taken to be equal to the orientation angle of the microcrack ϕ, for different normalized wave number ka for two values of a/d. For $a/d = 0.7$ (Fig. 4a), the lower frequency range $ka < 1$ results in a decrease in $|K^*|$ with increasing θ; $|K^*|$ approaches the static solution when $ka = 0$. For $ka > 1$, $|K^*|$ increases with a decreasing θ and remains almost constant when $ka = 1$. However, for $a/d = 0.9$ (Fig. 4b), higher interaction effects are in evidence at frequencies $ka \leqslant 1$ and $|K^*|$ approaches unity as ka increases to 1.5.

The effect of the microcrack orientation ϕ is examined in Figs 5(a) and 5(b). In Fig. 5(a), the left tip of the microcrack ($\eta = 0$, $\xi = -1$) is located at $y = 0$ and $x = e$, and the stress intensity factor for $e = 0.25a$ is plotted as a function of ϕ. The figure indicates that little change occurs with increasing ϕ up to 135° at which a rapid change in $|K^*|$ occurs. Figure 5(b), which relates to the case where the left tip of the microcrack is located at $y = e$ and $x = 0$, identifies the importance of frequency upon both shielding and amplification effects experienced by the main crack due to the presence of the microdefect.

It is worth pointing out that the normalized stress intensity factor $|K^*|$ presented in Figs 3–5 represents a dynamic amplification ratio of the stress intensity factor as a result of the presence of the microcrack. Since the effective stress intensity factor $|K_{III}|$ is described in terms of $|K^*|$ and $|K_0|$, then the dynamic overshoot phenomenon, observed for a single crack (Fig. 2), will be governed by the behaviour of $|K_0|$. Figure 6(a) shows an example of the variation of the normalized dynamic stress intensity factor of the main crack $|K_0|/K_{0s}$

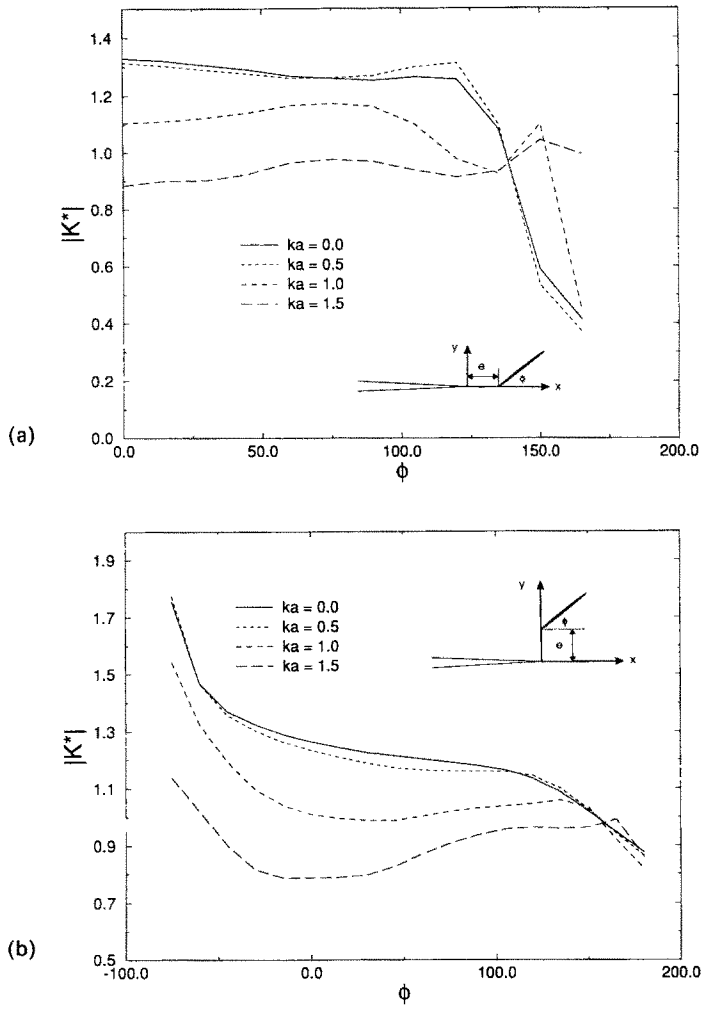

Fig. 5. Effect of microcrack orientation ϕ upon the dynamic stress intensity factor K^* for different frequencies: (a) $e/a = 0.25$; $e = d\cos\theta - a\cos\phi$ and (b) $e/a = 0.25$; $e = d\sin\theta - a\sin\phi$.

as a result of a distributed and concentrated harmonic load acting on its surface, such that $\tau_{yz}(x, 0) = -\tau H(x+l_0) + p\delta(x+l_0)$, where H is the step function, δ is the delta function and K_{0s} is the corresponding static stress intensity factor. The interaction of the above main crack with a collinear microcrack is shown in Fig. 6(b) for the case where $a/d = 0.9$, $\tau l_0/p = 1.0$ and K_s being the corresponding static result. These figures depict three important features: (i) the dynamic stress intensity factor attains a maximum value which exceeds that corresponding to the static case (dynamic overshoot), (ii) dynamic overshoot is also observed in the case involving a collinear microcrack interacting with a main crack, and (iii) the increase of the length of the collinear microcrack reduces the overshoot phenomenon.

4. CONCLUDING REMARKS

A general solution is provided to the dynamic interaction of a main crack with an arbitrarily located and oriented microcrack under antiplane loading. The analysis is based upon the use of integral transform techniques coupled with a self-consistent iterative procedure using Chebyshev polynomials.

The validity and versatility of the present solution have been demonstrated in a unified manner by application to some specific examples. Furthermore, the effect of location and

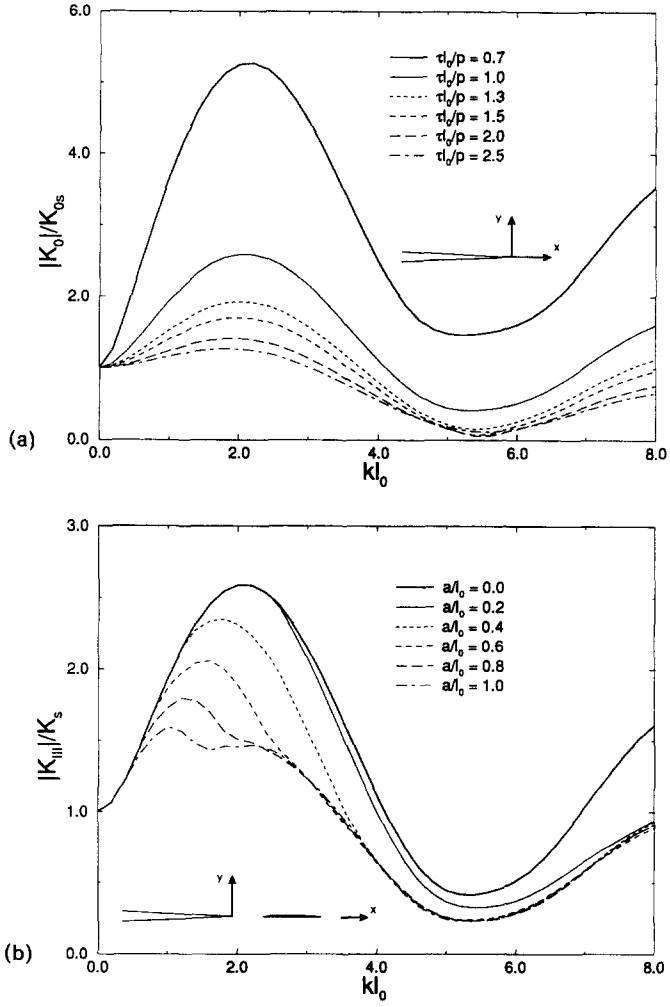

Fig. 6. Normalized stress intensity factor versus frequency for (a) a semi-infinite main crack under mode III loading, and (b) a main crack interacting with a collinear microcrack.

orientation of the microcrack and the frequency upon the dynamic stress intensity factor of the main crack are examined and discussed.

Acknowledgements—This work was supported in part by the Natural Sciences and Engineering Research Council of Canada and in part by Energy, Mines and Resources Canada and The University Research Incentive Fund of Ontario. The authors also acknowledge the constructive comments made by the reviewers.

REFERENCES

Achenbach, J. D. (1973). *Wave Propagation in Elastic Solids*. North-Holland, Amsterdam.

Chiang, C. R. (1986). The effect of an elliptical hole on the stress intensity factor of a macrocrack. *Engng Fracture Mech.* **25**, 17–21.

Claussen, N., Steeb, J. and Pabst, R. F. (1977). Effect of inducted microcracking on the fracture toughness of ceramics. *Bull. Am. Ceram. Soc.* **56**, 559–562.

Evans, A. G. and Faber, K. T. (1984). Crack-growth resistance of micro cracking brittle materials. *J. Am. Ceram. Soc.* **67**, 255–260.

Freund, L. B. (1990). *Dynamic Fracture Mechanics*. Cambridge University Press, Cambridge.

Gross, D. and Zhang, Ch. (1988). Diffraction of SH waves by a system of cracks: solution by an integral equation method. *Int. J. Solids Structures* **24**, 41–49.

Gong, S. X. and Meguid, S. A. (1991). A general solution to the antiplane problem of an arbitrarily located elliptical hole near the tip of a main crack. *Int. J. Solids Structures* **28**, 249–263.

Gong, S. X. and Meguid, S. A. (1992). Microcrack interaction with a main crack: a general treatment. *Int. J. Mech. Sci.* **34**, 933–945.

Hoagland, R. G., Hahn, G. T. and Rosenfield, A. R. (1973). Influence of microstructures on the fracture propagation in rock. *Rock Mech.* **5**, 77–106.

Hoagland, R. G. and Embury, J. D. (1980). A treatment of inelastic deformation around a crack tip due to microcracking. *J. Am. Ceram. Soc.* **63**, 404–410.

Hutchinson, J. W. (1987). Crack tip shielding by micro-cracking in brittle solids. *Acta Metall.* **35,** 1605–1619.
Itou, S. (1980). Diffraction of an antiplane shear wave by two coplanar Griffith cracks in an infinite elastic medium. *Int. J. Solids Structures* **16,** 1147–1153.
Jain, D. L. and Kanwal, R. P. (1972). Diffraction of elastic waves by two coplanar Griffith cracks in an infinite elastic medium. *Int. J. Solids Structures* **8,** 961–975.
Krajcinovic, D. (1985). Continuous damage mechanics revisited: basic concepts and definitions. *J. appl. Mech.* **52,** 829–834.
Kachanov, M. (1987). Elastic solids with many cracks: a simple method of analysis. *Int. J. Solids Structures* **23,** 23–44.
Meguid, S. A., Gong, S. X. and Gaultier, P. E. (1991). Main crack–microcrack interaction under mode I, II and III loadings: shielding and amplification. *Int. J. Mech. Sci.* **33,** 351–359.
Ortiz, M. (1987). Continuum theory of crack shielding in ceramics. *J. appl. Mech.* **54,** 54–58.
Rose, L. K. F. (1986). Microcrack interaction with a main crack. *Int. J. Fract.* **31,** 233–242.
Ruhle, M., Evans, A. G., McMeeking, R. M., Charalambides, P. G. and Hutchinson, J. W. (1987). Microcrack toughening in alumina/zirconia. *Acta Metall.* **35,** 1701–1710.
Zhang, Ch. and Achenbach, J. D. (1989). Time-domain boundary element analysis of dynamic near-tip fields for impact-loaded collinear cracks. *Engng Fracture Mech.* **32,** 899–909.
Zhang, Ch. (1992). Elastodynamic analysis of a periodic array of mode III cracks in transversely isotropic solids. *J. appl. Mech.* **59,** 366–371.

APPENDIX

The Fourier transform used in this paper is defined as

$$\bar{f}(s)=\frac{1}{2\pi}\int_{-\infty}^{\infty} f(x)\,e^{isx}\,dx, \quad f(x)=\int_{-\infty}^{\infty}\bar{f}(s)\,e^{-isx}\,ds. \tag{A1}$$

The following results are used in calculating the integrals corresponding to eqns (31) and (32)

$$\int_0^{\infty} J_k(as)\cos(s|x|)\,e^{-s|y|}\,ds=\frac{a^k\cos\left(Ak-\dfrac{|B|}{2}\right)}{R\left[\left(R\cos\dfrac{|B|}{2}+|y|\right)^2+\left(R\sin\dfrac{|B|}{2}+|x|\right)^2\right]^{k/2}}, \tag{A2}$$

$$\int_0^{\infty} J_k(as)\sin(s|x|)\,e^{-s|y|}\,ds=\frac{-a^k\sin\left(Ak-\dfrac{|B|}{2}\right)}{R\left[\left(R\cos\dfrac{|B|}{2}+|y|\right)^2+\left(R\sin\dfrac{|B|}{2}+|x|\right)^2\right]^{k/2}}, \tag{A3}$$

where

$$R=4\sqrt{(y^2-x^2+a^2)^2+4x^2y^2}$$

$$B=-\left|\arccos\frac{y^2-x^2+a^2}{R^2}\right|$$

$$A=-\arctan\frac{R\sin\dfrac{|B|}{2}+|x|}{R\cos\dfrac{|B|}{2}+|y|}.$$